SLC4A10 mutation causes a neurological disorder associated with impaired GABAergic transmission

James Fasham[1,2†], Antje K. Huebner[3†], Lutz Liebmann[3†], Reham Khalaf-Nazzal[4†], Reza Maroofian[5], Nderim Kryeziu[3], Saskia B. Wortmann[6,7,8,] Joseph S. Leslie[1], Nishanka Ubeyratna[1], Grazia M.S. Mancini[9], Marjon van Slegtenhorst[9], Martina Wilke[9], Tobias B. Haack[10], Hanan Shamseldin[11], Joseph G. Gleeson[12,13], Mohamed Almuhaizea[14], Imad Dweikat[4], Bassam Abu-Libdeh[15], Muhannad Daana[16], Maha S. Zaki[17], Matthew N Wakeling[1], Lucy McGavin[18], Peter D. Turnpenny[1,2], Fowzan S. Alkuraya[11], Henry Houlden[5], Peter Schlattmann[19], Kai Kaila[20,21] , Andrew H. Crosby[1‡], Emma L. Baple[1,2‡], Christian A. Hübner[3,22‡]

[†]**These authors contributed equally to this work.**

[‡]**Co-corresponding authors**

Author affiliations:

1. RILD Wellcome Wolfson Centre, University of Exeter Medical School, Royal Devon and Exeter Hospital, Exeter EX2 5DW, UK
2. Peninsula Clinical Genetics Service, Royal Devon University Healthcare NHS Foundation Trust, Exeter EX2 5DW, UK
3. Institute of Human Genetics, Jena University Hospital, Friedrich Schiller Universität, Am Klinikum 1, 07747, Jena, Germany
4. Faculty of Medicine, Arab American University of Palestine, Jenin, P227, Palestine
5. Molecular and Clinical Sciences Institute, St. George's University of London, London, UK
6. University Children's Hospital, Salzburger Landeskliniken (SALK) and Paracelsus Medical University (PMU), 5020 Salzburg, Austria
7. Amalia Children's Hospital, Radboudumc, Nijmegen, The Netherlands
8. Institute of Human Genetics, Technische Universität München, Munich, Germany
9. Department of Clinical Genetics, Erasmus Medical Center, room Ee2077, Dr Molewaterplein 40. 3015 GD Rotterdam, The Netherlands
10. Institute of Medical Genetics and Applied Genomics, University of Tuebingen, 72076 Tübingen, Germany
11. Department of Translational Genomics, Center for Genomic Medicine, King Faisal Specialist Hospital and Research Center, Riyadh, Saudi Arabia
12. Rady Children's Institute for Genomic Medicine, San Diego, USA

13. Department of Neurosciences, University of California, San Diego, USA
14. Department of Neuroscience, King Faisal Specialist Hospital and Research Center, Riyadh, Saudi Arabia
15. Department of Pediatrics and Genetics, Makassed Hospital and Al-Quds University, East Jerusalem, 95908, Palestine
16. Department of Pediatrics, Arab Women's Union Hospital, Nablus, P400, Palestine
17. Clinical Genetics Department, Human Genetics and Genome Research Division, National Research Centre, Cairo, Egypt.
18. Department of Radiology, Derriford Hospital, Plymouth, UK
19. Institute for Medical Statistics, Computer Science and Data Science, Jena University Hospital, Jena, Germany
20. Molecular and Integrative Biosciences, University of Helsinki, 00014 Helsinki, Finland
21. Neuroscience Center, Helsinki Institute of Life Science, University of Helsinki, 00014 Helsinki, Finland
22. Center for Rare Diseases, Jena University Hospital, Friedrich Schiller Universität, 07747 Jena, Germany

Supplemental Material

Detailed clinical case descriptions

Family 1, III:1 and 2

Two male siblings were born to unaffected first cousin Palestinian parents. The elder brother (III:1) was a product of an uncomplicated pregnancy and delivery, but presented profoundly hypotonic at birth, requiring immediate and sustained respiratory support. He suffered a single afebrile seizure aged 1 year of age for which he has not required further treatment. His development was delayed, he bottom shuffled then walked after two years. Aged eight years and seven months, he could walk and run, feeds himself with his hands and is toilet trained but has only eight words. He displays behaviors suggestive of an autistic spectrum disorder condition including hyperactivity, aggressive episodes and anxiety that have required residential care, and treatment with methylphenidate and risperidone. His younger brother (III:2), also the product of an uncomplicated pregnancy and delivery was initially discharged home where he suffered a cyanotic episode at three weeks of age, possibly a seizure, requiring urgent readmission. His development was profoundly delayed, walking at five years of age. Now aged seven years eight months he has no language, either spoken or receptive, poor fine motor skills and is not toilet trained. He is less aggressive than his sibling but exhibits stereotyped hand-flapping. Both brothers have been hospitalized on multiple occasions

with upper and lower respiratory tract infections. Both are brachycephalic and microcephalic and with large, rotated ear lobes and hypotelorism. The younger child has inverted nipples. On neurological examination, both displayed axial hypotonia, peripheral spasticity and exaggerated deep tendon reflexes. MRI neuroimaging of both siblings showed slit lateral ventricles and a dysmorphic, thickened, flattened corpus callosum, which was associated with an unusual configuration of the midline structures (fornices and septum pellucidum) (**Fig. 2**).

Family 2, II:1

This boy was the only child born to unrelated Austrian parents. He was severely hypotonic in the neonatal period with poor suck, resulting in faltering growth and delayed acquisition of motor milestones, rolling first at three-and-a-half years. He has mild craniofacial dysmorphism with an elongated face, prominent metopic ridge, tent-shaped mouth with long philtrum, low-set large ears and tapering fingers. Skeletal anomalies include bilateral *coxa vara anteverta* and left developmental dysplasia of the hip requiring surgical remediation. At age four years and eight months he has severe global developmental delay (virtually non-ambulatory, babbles only, no speech), severe central and peripheral hypotonia, severe failure to thrive but no microcephaly. MRI neuroimaging at 10 months of age, reported by the local radiologist, showed slit lateral ventricles (first seen on neonatal cranial ultrasound) with generalized cerebral volume loss and a hypoplastic corpus callosum (**Fig. 2**). Myelination appears appropriate for age.

Family 3, II:2 and II:3

Two sisters from Saudi Arabia, born at term, presented with profound hypotonia in infancy, microcephaly and global developmental impairment.

The elder sister (II:2), now 12 years of age, has severe neurodevelopmental delay – she did not crawl until 3 years of age, and now sits only with support. Her fine motor skills are profoundly delayed and she still uses a palmar grasp. She is not reaching and shows no interest in play with toys. She has some behaviors associated with autistic spectrum disorder, including hand flapping and head nodding with preference of holding papers and difficulty in bathing. She is affected by generalized tonic-clonic seizures, first apparent at age seven and now occurring approximately monthly and lasting from 2 to 5 minutes. Inter-ictal EEG performed in 2016 showed background slowing. She was born with bilateral ankle contractures and bilateral foot deformities. Over time a left esotropia became apparent.

The younger sister (II:3) required nasogastric feeding in the first week of life and has progressed to severe global developmental delay and cognitive impairment with microcephaly, but without apparent seizures.

Additionally lambdoid craniosynostosis and ankle contractures are present in the younger child. She is fully dependent on her caregiver. MRI neuroimaging of the younger sibling revealed small lateral ventricles with normal external CSF spaces and appropriate myelination. The corpus callosum and midline structures are within normal range (**Fig. 2**).

Previous unremarkable investigations include, very long chain fatty acids, acylcarnitine profile and serum amino acids in both. Additionally, magnetic resonance spectroscopy (MRS), urine organic acids thyroid stimulating hormone, biotinidase levels and genetic tests for myotonic dystrophy and Prader Willi syndrome in the younger sibling.

Trio WES of the elder sister (II:2) was undertaken as part of a large-scale, first-tier clinical exome sequencing study (Monies *et al.* 2019 - ID: 17-4393) using methods and variant filtering strategies previously described. This identified a homozygous *SLC4A10* canonical splice acceptor site variant as the most likely cause of disease [Chr2(GRCh38):g.161964133A>C; NM_001178015:c.2863-2A>C]. The variant, which was confirmed by rtPCR of mRNA extracted from blood of an both affected individuals, which identified an additional band, representing mRNA with partial inclusion of intron 21 leading to premature stop after 13 additional amino acids [p.(Gln954_Phe955ins*13)] (**Supplementary Fig. 3**), Individual II:3 was confirmed to be homozygous for the same *SLC4A10* variant using Sanger sequencing performed locally.

Family 4; III:2, III:3 and III:5

This extended Egyptian family consists of two affected brothers (ten years of age and six years three months) and their affected female double first cousin (seventeen years, five months). All were born at term with normal birth weight and are now of proportionate short stature and low weight with disproportionately severe postnatal microcephaly (-4 to -6 standard deviations; SDS). All affected individuals have severe developmental impairment, first walking between six and seven years and two developed a broad-based gait (III:3 and III:5). All were non-verbal with extremely limited receptive language (cannot follow one-step commands or identify body parts). Behavioral abnormalities included hyperactivity and features associated with autistic spectrum disorder. Neurological findings were consistent across all affected individuals and included global hypotonia, with normal deep tendon reflexes and plantar responses. No individuals suffered clinical seizures, but an electroencephalogram (EEG) in Individual III:2 noted bitemporal epileptogenic discharges at the age of five years that resolved without treatment. Neuroimaging was not available for review. Ophthalmological examination, including visual evoked potentials (VEP) and

electroretinogram (ERG) was normal in Individual III:2 and hearing assessment, measured by auditory brainstem response (ABR).

Family 5; II:1 and 2.

These two Turkish children presented with hypotonia, global developmental impairment and microcephaly. The elder sister is more mildly affected; she walked aged two and at the age of 10-11 years her speech was dysarthric, she struggles to hold a pen and has an IQ around 53. At the age of 15 years she attends school for special needs education with a developmental level comparable to a seven-year-old child and is described as quite sociable. She has mild dysmorphic features (a prominent forehead and arched eyebrows) joint laxity, an accessory nipple, and fetal finger pads. The younger brother is more severely affected; he is severely microcephalic, walked at aged three years, has no speech and cannot feed himself at six years of age. He has brachycephaly with a forehead upsweep, arched eyebrows with flat orbital ridges and a bulbous nasal tip and prognathism. He has central hypotonia but peripheral hypertonia with brisk reflexes and a positive Babinski's sign. MRI neuroimaging of the brother identified a short and thick corpus callosum with hypoplastic pons and brainstem, normal myelination, lateral ventricles with collapsed anterior horns (**Supplementary Fig. 5d-f**). His sister's imaging was similar, without the dysmorphic appearance of the corpus callosum (**Supplementary Fig. 5a-c**). Both had mildly increased excretion of creatine, with other metabolic investigations reported normal.

Reference for Family 3

Monies D, Abouelhoda M, Assoum M, Moghrabi N, Rafiullah R, *et al.* Lessons Learned from Large-Scale, First-Tier Clinical Exome Sequencing in a Highly Consanguineous Population. Am J Hum Genet. 2019 Jun 6;104(6):1182-1201.

Supplementary Figure 1: Genome sequencing data of affected individuals in Family 1, revealing a biallelic, multi-exon, deletion of *SLC4A10*.

Integrative genome viewer (IGV) plots illustrating the homozygous deletions in *SLC4A10* in Family 1; III:1 [*top panel*] and III:2 [*middle panel*] shown alongside a wild-type control sequence obtained under the same conditions [*bottom panel* read alignment over the deleted region]. The deletion was confirmed using ddPCR (**Supplementary Fig. 2**).

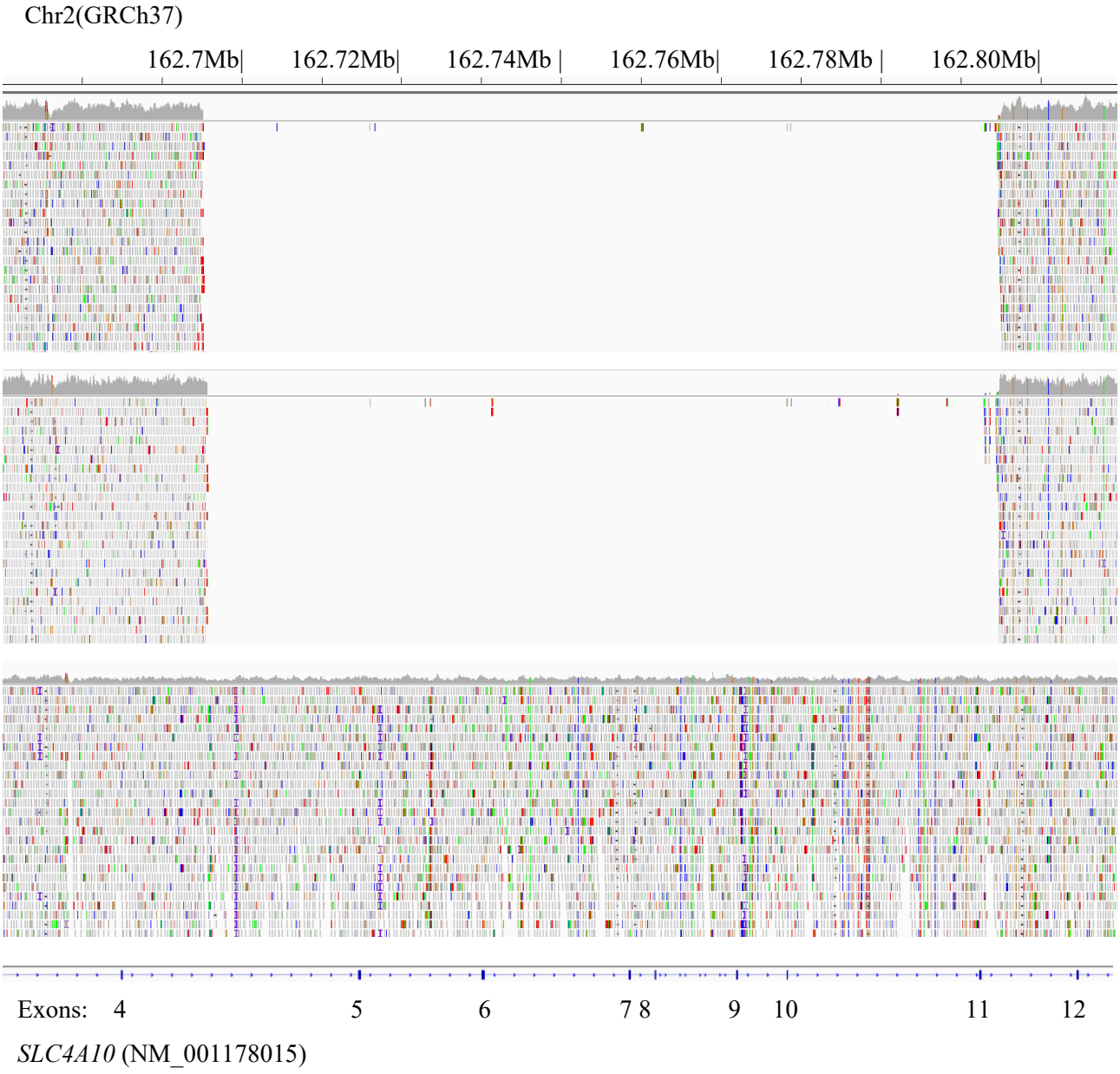

Supplementary Figure 2: ddPCR data confirming the presence of a multi-exon deletion of *SLC4A10* in individuals III:1 and III:2 (Family 1)

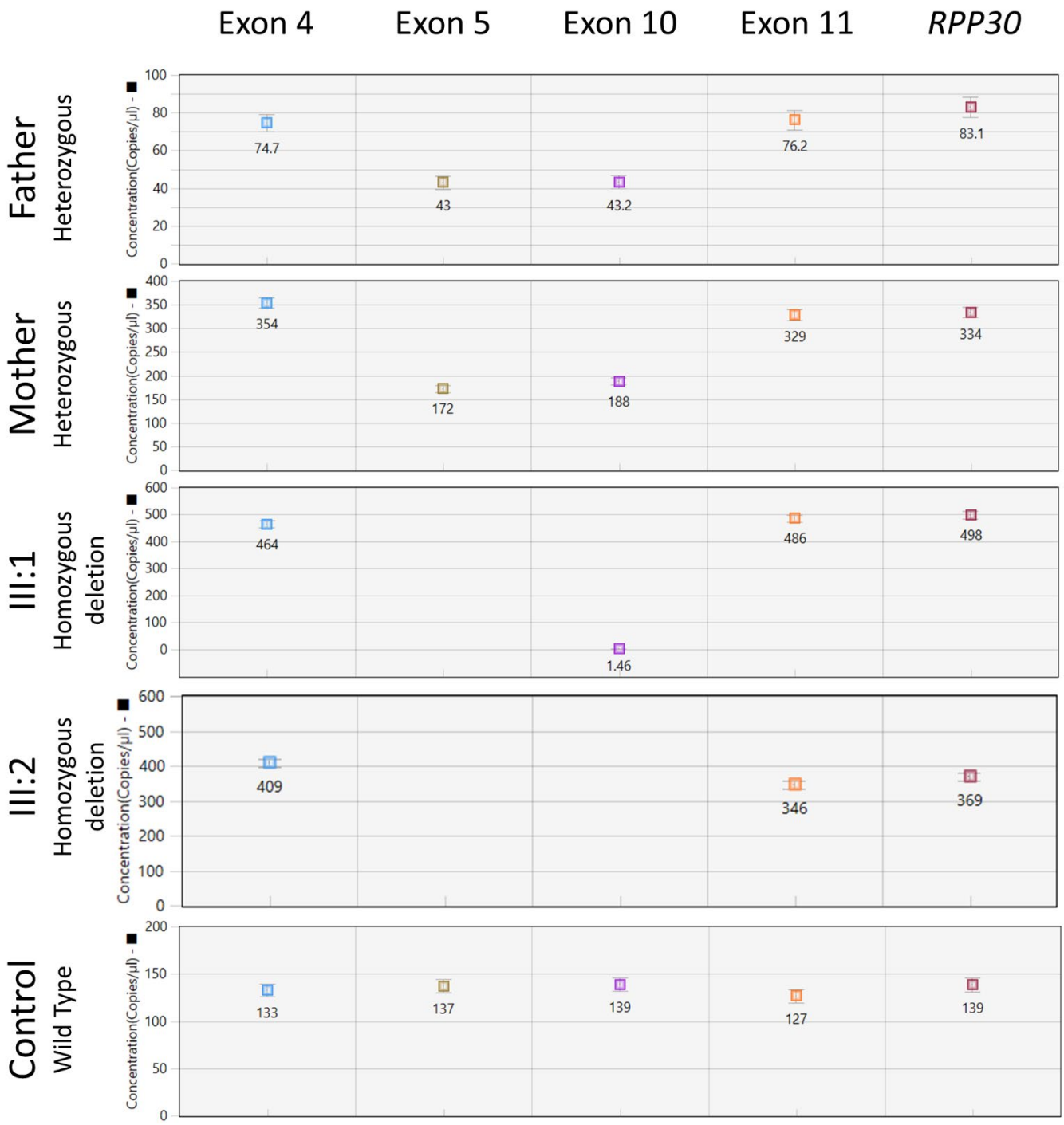

Primer Sequences: Conditions: 59 degrees

Exon4_Forward: TTCTTGGAACCGAGGATGAT

Exon4_Reverse: CTTCACGCCAACAAATCTCA

Exon5_Forward: GAAAGGTGGAGCAAGCCTTA

Exon5_Reverse: GCATGTCCAGCAACACAGTT

Exon10_Forward: CAGGAATTGATGAGTTTCTGGA

Exon10_Reverse: CTGGGAAGGAACATTTTTGG

Exon11_Forward: ACTCTCCACAGGAGAAGAGGA

Exon11_Reverse: TGGTCCTTGAAGTCCCATAGA

RPP30_Forward: GGGCCCTTTTCTTTGGTTGT

RPP30_Reverse: TCCCAACCTTCCAAGCTGAT

Supplementary Figure 3: RT-PCR demonstrating mRNA splicing effect of NM_001178015:c.2863-2A>C p.(Gln954_Phe955ins*13) variant (Family 3).

A) Simplified gene intron-exon structure of *SLC4A10* showing splicing effect of the c.2863-2A>C variant (red dashed line). This variant weakens the splice acceptor site (red dashed line), leading to the preferential usage of a more 3' acceptor site (solid red line) with the resultant deletion of 9bp from the start of exon 22 (red shaded region). This also affects the donor site, with an alternative more 3' site utilised (blue solid line) in preference to the canonical site (blue dashed line). The use of the alternative splice donor site results in the retention of 175 bp of intron 21 (shaded blue) resulting in 13 additional amino acids being included before a premature stop codon (red octagon).

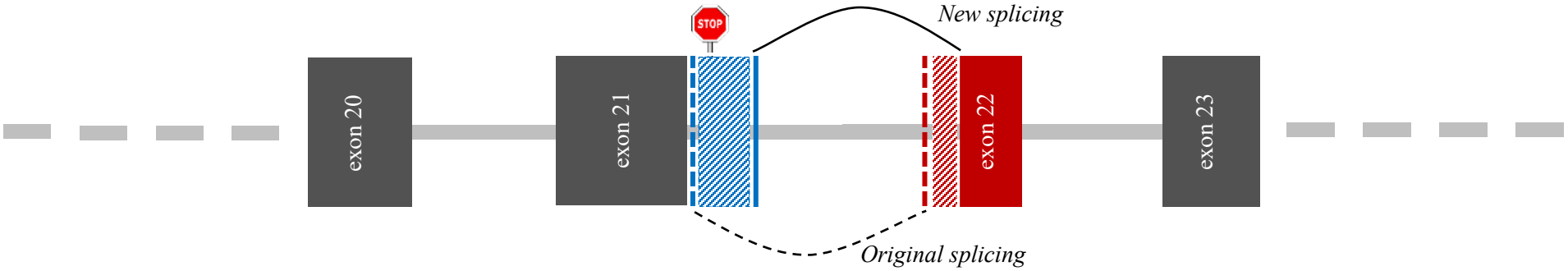

B) SLC4A10 mRNA sequence obtained from peripheral blood of an affected individual. Grey highlighting indicates nucleotides derived from exons 21 and 22. Blue highlighting indicates bases derived from the retention of intron 21. Red text in square brackets indicates the deleted sequence at the start of exon 22. Codon phase is shown with alternating text colour until the premature stop codon (red text, with blue highlighting).

TTTATTCCCATGCCAGTGCTATATGGAGTGTTTCTTTATATGGTGCTTCATCTCTAAAGGGAATTCAG | *(start of retained intron)*
GTAAATTACTTACAGTACTACAGGCACATCTGTGATGACTGACCTTAAGGTCTACTGATAAGTCATGTGACAGCTGAGAAAATGCCACCACCTGA
GGAACAGCTTTTAGACCACAATTAAATTTCTTCAAACTTGTCAGAGTTACAAAAGTTAAAGAAGATTCTCTCCAGCATCT | *(new splice site)*
[TTCTTTGAT]AGGATAAAGCTCTTCTGGATGCCGGCAAAACATCAACCAGATTTTATATACCTAAGGCACGTACCGCTTCGAAAAGTGCATCTCTT
CACAATTATTCAGATGAGTTGCCTTGGCCTTTTGTGGATAATAAAAGTTTCAAGAGCTGCTATTGTCTTTCCCATGATG

C) Chromatogram demonstrating the retention of part of intron 21 in an affected individual (blue dotted line).

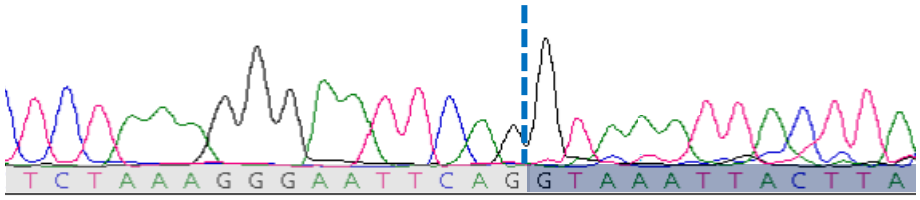

Supplementary Figure 4: T2-weighted sagittal MRI scan of wild type and *SLC4A10* knockout mice.

Whilst lateral ventricles (arrowheads) are seen in the wild type mouse (left), these are not macroscopically apparent in the knockout mouse (right) suggesting a marked reduction in volume.

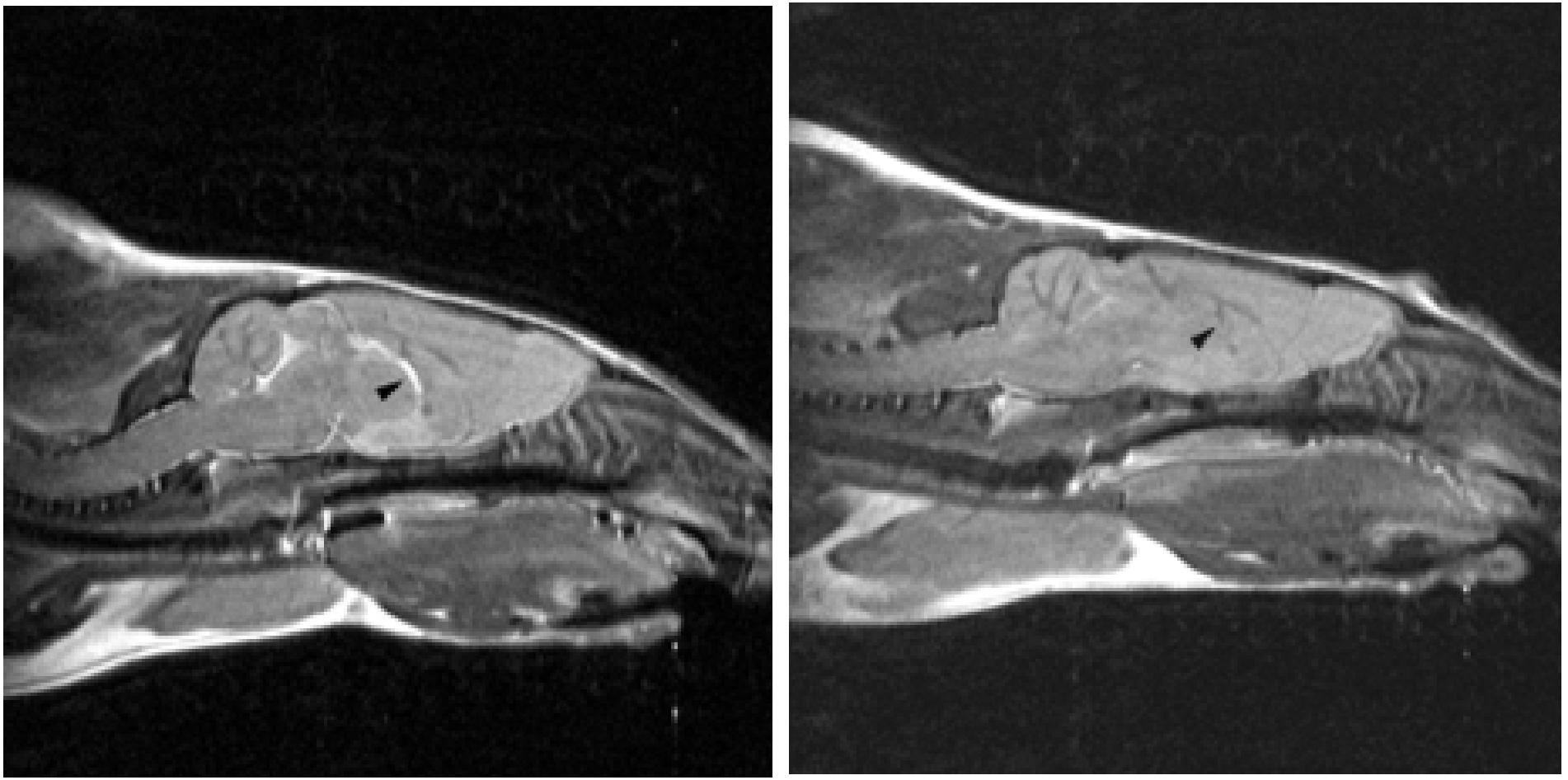

Supplementary Figure 5: Additional MRI images of individuals affected by SLC4A10-related disorder.
All images made available to the authors are shown.

Top row Family 5, Individual II:1 (female) 2 years 2 months, showing slit-like anterior horns of the lateral ventricles
A,B) T2 axial **C)** T2 sagittal (midline)
Middle Row Family 5, Individual II:2 (male) 2 years 7 months showing a dysplastic corpus callosum.
D,E) T1 axial **F):** T1 sagittal (midline)

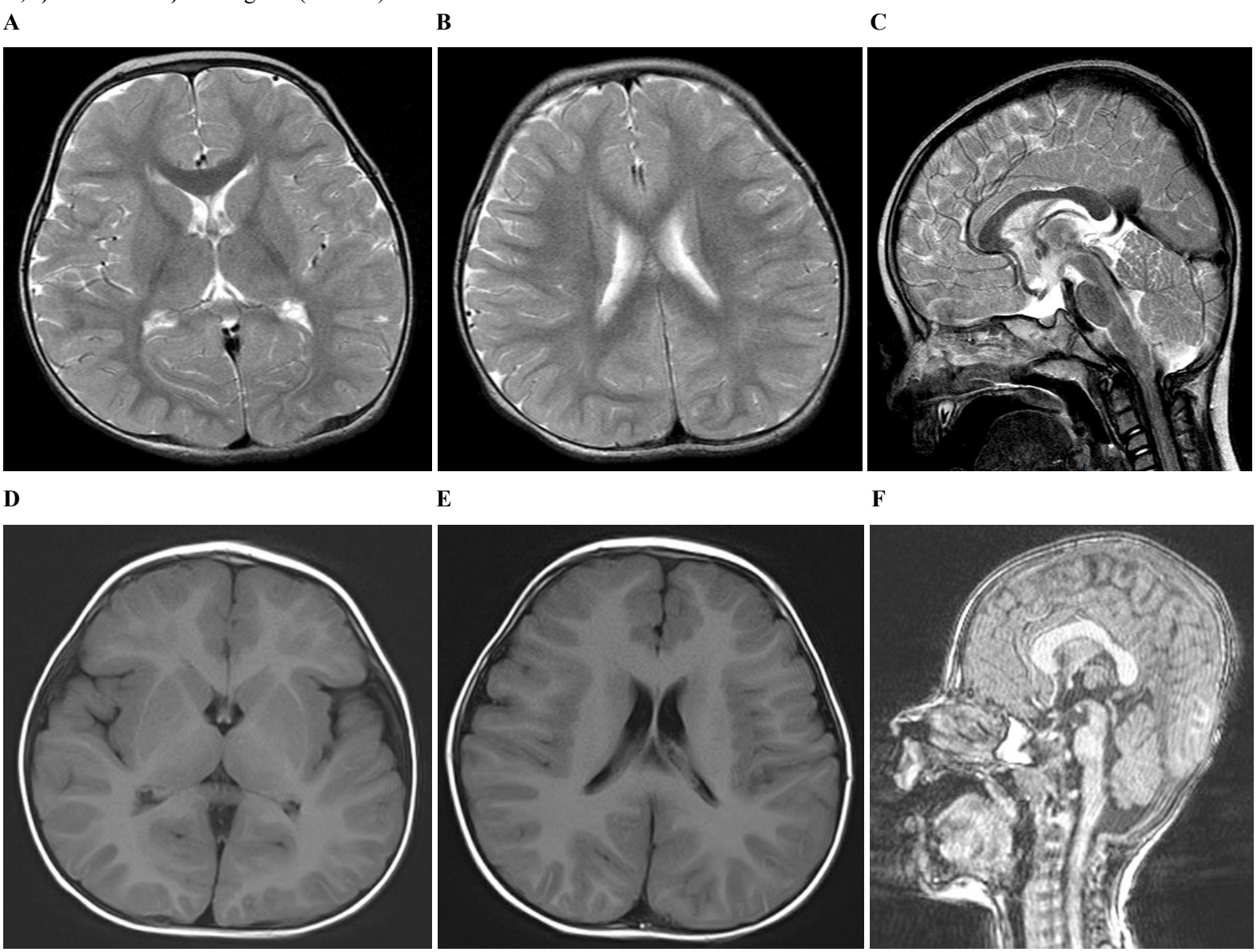

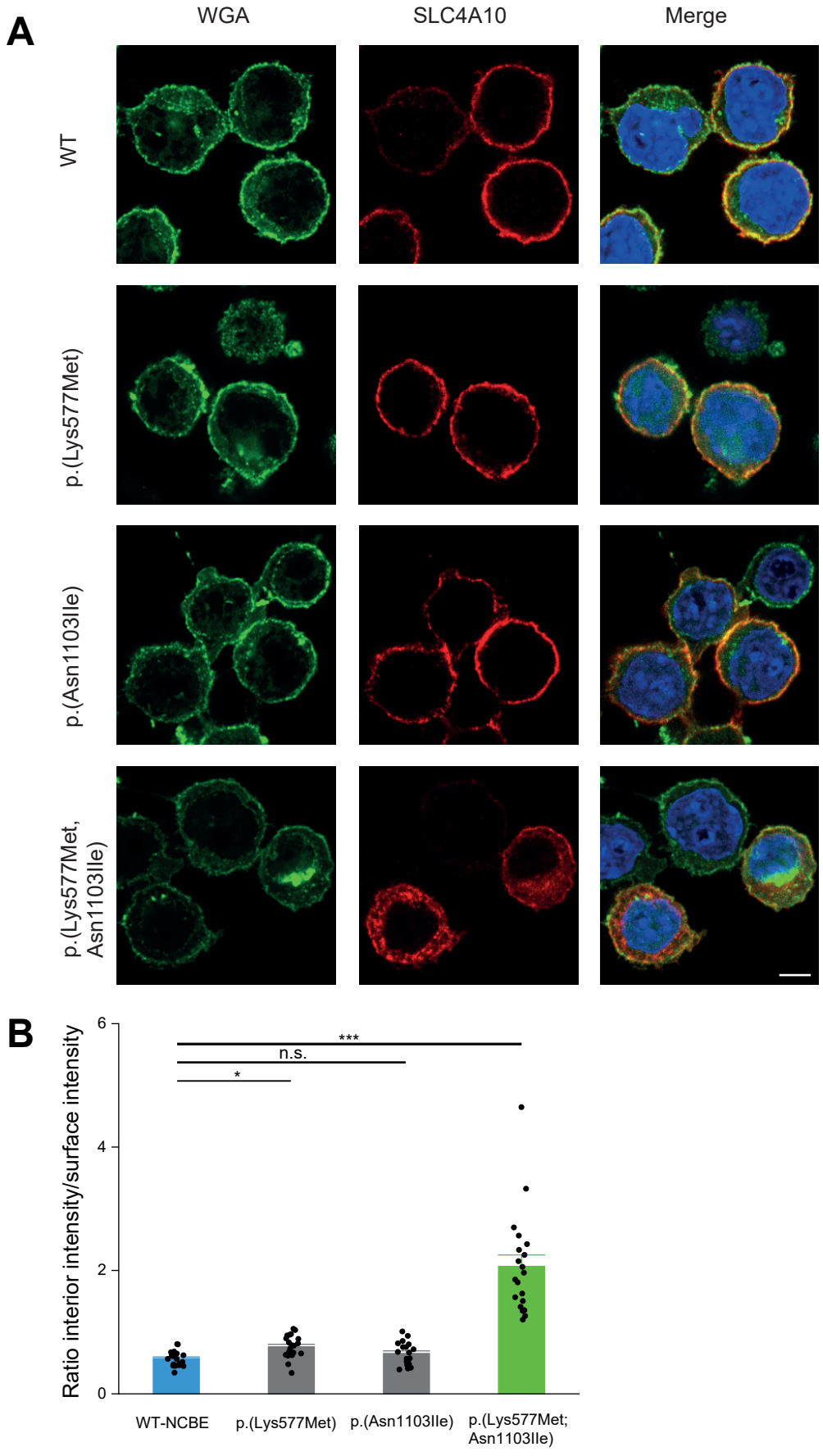

Supplementary Figure 6: Heterologous expression of SLC4A10 wildtype (WT) and disease associated missense variants in N2a cells.

A) Two days post-transfection into the fast-growing mouse neuroblastoma cell line N2a, cells were fixed with 4% PFA and stained with an antibody directed against an N-terminal epitope of SLC4A10 and with the lectin wheat germ agglutinin (WGA) to label glycan structures associated with the Golgi apparatus or the plasma membrane. Cells transfected with the wild-type SLC4A10 construct display a predominant SLC4A10 labelling at the plasma membrane. While either the variant protein p.(Lys577Met) or p.(Asn1103Ile) were still targeted to the plasma membrane, the p.(Lys577Met; Asn1103Ile) variant was partially retained intracellularly. Scale bar: 1 µm.
B) Quantification of the ratio of interior versus surface intensity of the SLC4A10 signal. n=12 cells each. Bootstrap F-test with posthoc bootstrap t-test. n.s. not significant,* $p<0.05$, *** $p<0.001$.

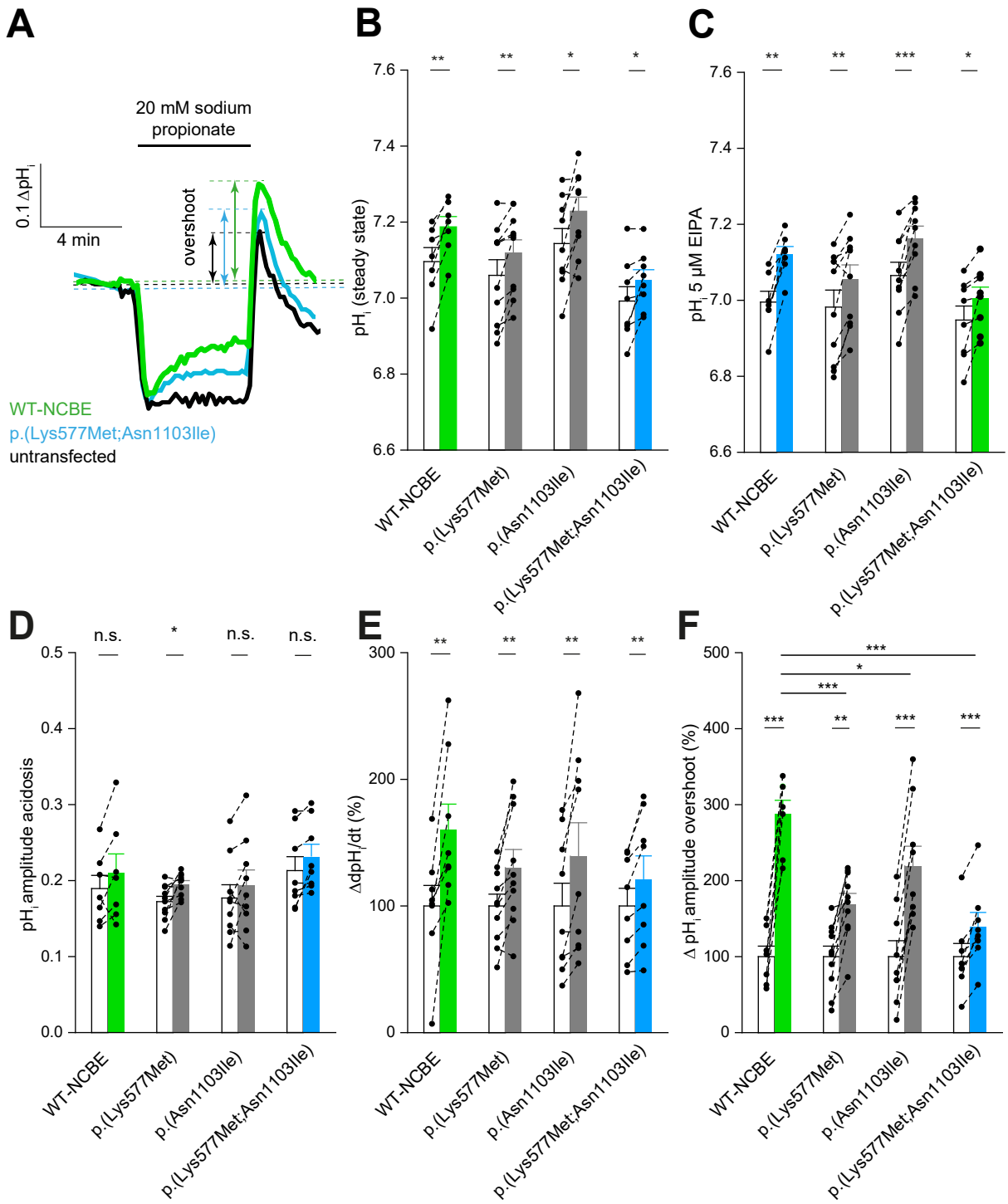

Supplementary Figure 7: Acid extrusion by disease associated SLC4A10 missense variants is compromised.

A) Representative single cell pHi traces obtained in an untransfected N2a cell, a cell transfected with SLC4A10 (NCBE) WT and a cell transfected with the p.(Lys577Met;Asn1103Ile) variant superfused with bicarbonate-buffered solution with 5 µM EIPA to block Na+/H+ exchange. Cells were acidified by a 5 min 20 mM sodium propionate pulse. Calibration was performed with the high-$[K^+]_o$/nigericin technique.

B,C) The pHi of transfected N2a cells construct was slightly more alkaline compared to untransfected cells at steady state (b) and in the presence of 5 µM EIPA (c).

D) The amplitude of pHi change in response to the sodium propionate pulse did not differ between transfected and untransfected cells.

E) The recovery from the acid load did not differ between cells transfected with different SLC4A10 constructs tested.

F) The amplitude of the overshoot was reduced for p.(Lys577Met), p.(Asn1103Ile) and the combination of both.

Mean+SEM from 6 independent experiments with more than 60 cells analysed (bootstrap t-test / bootstrap F-test (f); n.s.: not significant; * $p<0.05$; ** $p<0.01$; *** $p<0.001$)

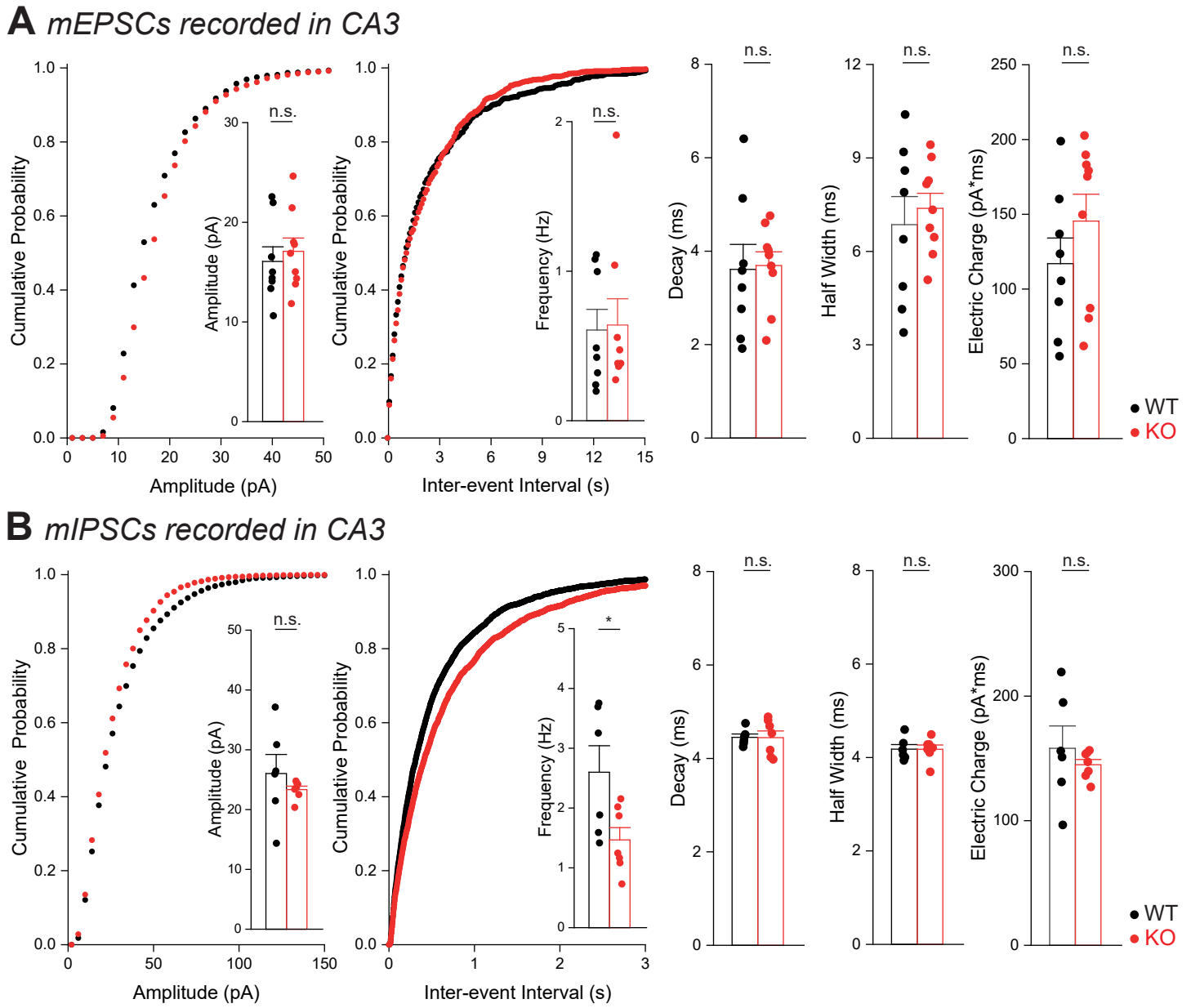

Supplementary Figure 8: Disruption of Slc4a10 reduces the mIPSC frequency in CA3 pyramidal neurons.

A) Glutamatergic transmission is not altered in CA3 neurons of Slc4a10 KO mice. Cumulative plots and bar charts of mEPSC properties. No significant differences were detected in mEPSC frequency,amplitude or kinetics (n= 8/9; bootstrap t-test; n.s.: not significant).

B) The mIPSC frequency is diminished in CA3 neurons of Slc4a10 KO mice in the presence of bicarbonate. Cumulative plots and bar charts of mIPSC properties (n=6/7; Mean+SEM; bootstrap t-test; n.s.: not significant).

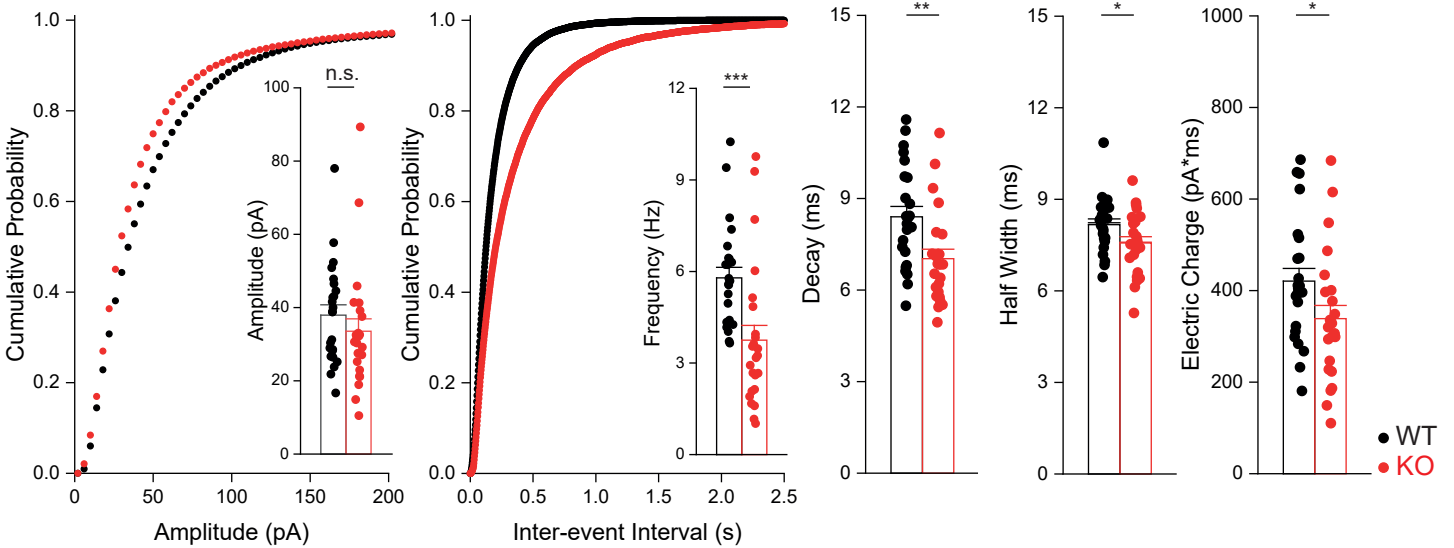

Supplementary Figure 9: Disruption of Slc4a10 reduces the sIPSC frequency in CA1 pyramidal neurons

Cumulative plots and bar charts of different sIPSC properties. The sIPSC frequency was diminished in CA1 neurons of Slc4a10 KO mice in the presence of bicarbonate (n=21/22; Mean+SEM; bootstrap t-test: * $p<0.05$; ** $p<0.01$; *** $p<0.001$; n.s.: not significant).

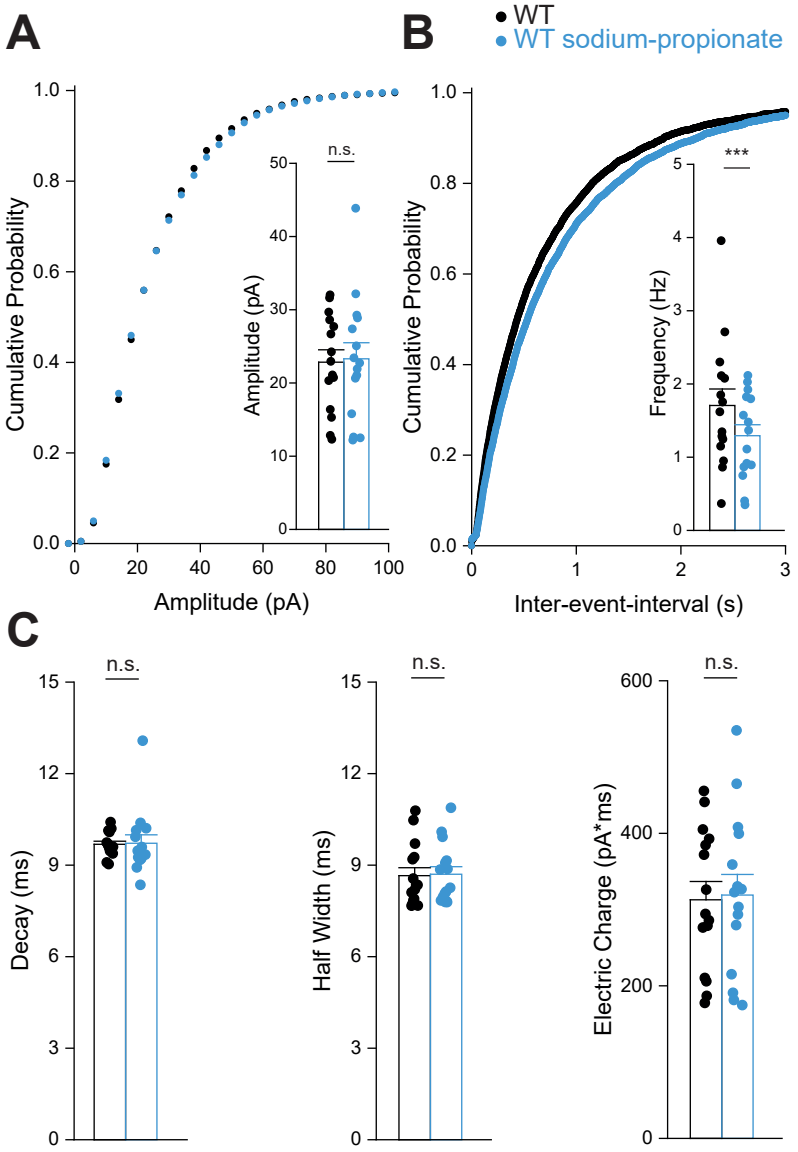

Supplementary Figure 10: Intracellular acidification with sodium propionate impairs GABA release.

A) In acute wild-type brain slices the mean mIPSC amplitude did not change upon substitution of 20 mM NaCl by sodium propionate.
B) mIPSC frequency was significantly diminished in the presence of 20 mM sodium propionate.
C) τ-decay, half-width and transported electric charge were not affected by sodium propionate.

n=15 cells each; Mean+SEM; bootstrap paired t-test: ***p<0.001; n.s.: not significant.

Supplementary Figure 11: Protein modelling of missense SLC4A10 variants.

SLC4A10 p.(Lys577Met) [red] shown on 3.5 Å resolution, x-ray crystallographic structure of dimeric human SLC4A1 (4yzf)[residues 486 – 1037]. SLC4A1 is a paralogue of SLC4A10 with 41% sequence identity. The two dimeric chains are shown in light and dark grey. The change from a charged residue to a hydrophobic residue may impact positioning of the protein within the cell membrane [approximate position - blue].

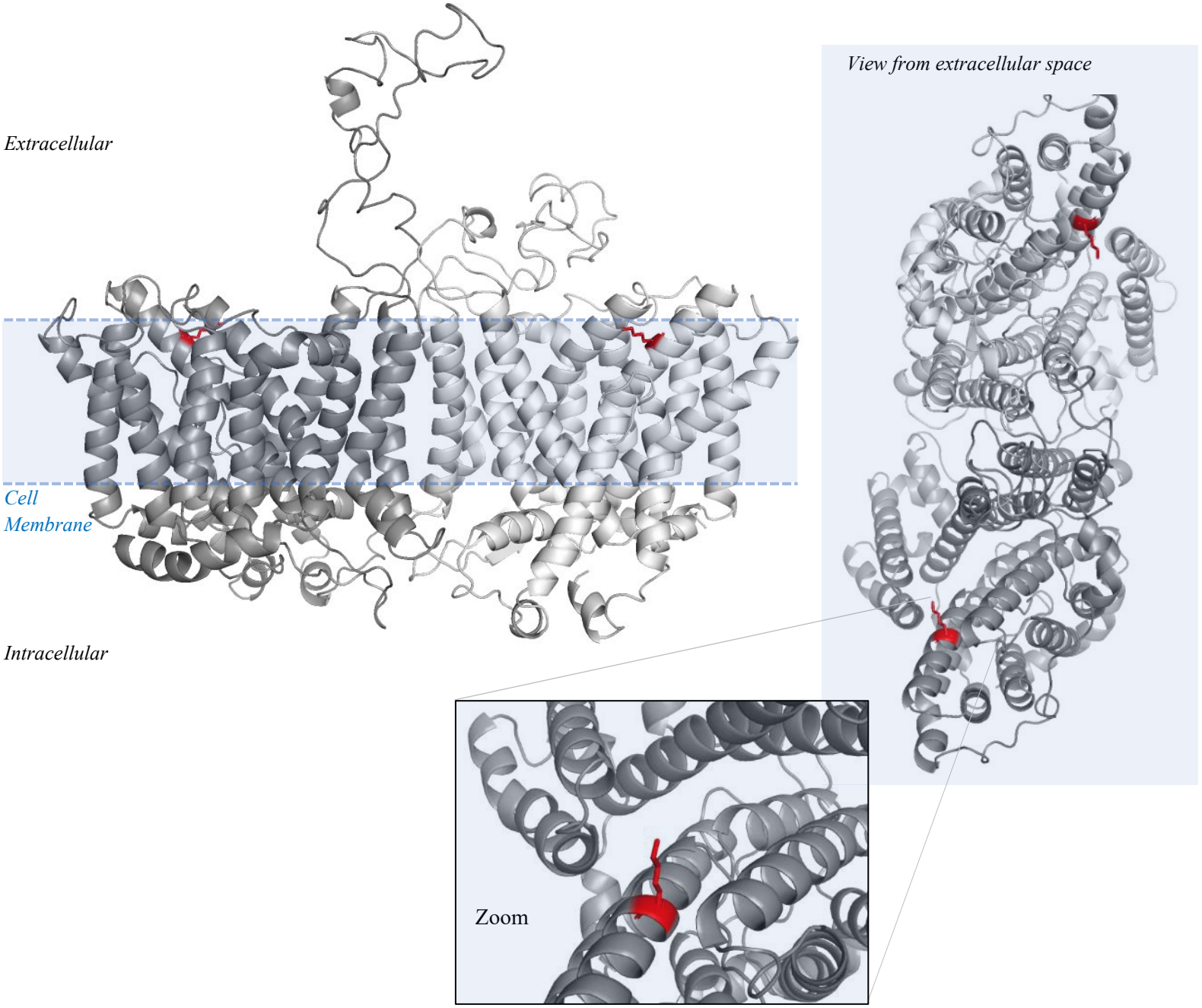

Supplementary Table 1: Human and murine disorders associated with other SLC4A class molecules.

Gene	Expression	Function	OMIM disorder	Inh	Human (not in OMIM)	Mouse
SLC4A1 (AE1)	Blood, Kidney	mediates exchange of chloride and bicarbonate across the phospholipid bilayer and plays a central role in respiration of carbon dioxide.	Cryohydrocytosis	AD		Severe spherocytosis and hemolysis[1,2]
			Distal renal tubular acidosis 1	AD		
			Distal renal tubular acidosis 4 with hemolytic anemia	AR		
			Ovalocytosis, SA type	AD		
			Spherocytosis, type 4	AD		
SLC4A2 (AE2)	Many	nonerythroid anion exchanger	-	-	low phospholipid-associated cholelithiasis[3]	male, but not female -/- mice, infertile with histopathologic evidence of interruption in spermiogenesis[4]
SLC4A3 (AE3)	Heart, Ovary, others	electroneutral Cl^- /HCO_3^- exchanger	-	-	Short QT syndrome[5] Idiopathic generalized epilepsy: increase in frequency of 867Asp variant in patients vs. controls [6]	Reduced seizure threshold and increased seizure-induced mortality[7] Double-knockout mice (with Nkcc1 (SLC12A2)) showed impaired cardiac contractility.[8]
SLC4A4 (NBC1)	Brain, Pancreas, Kidney	transport of Na and HCO_3^- out of the corneal stroma and into the aqueous humor	Renal tubular acidosis, proximal, with ocular abnormalities[9]	AR	-	-
SLC4A5 (NBC4)	Thyroid, Testis (brain)	electrogenic, chloride-independent, stilbene-inhibitable sodium bicarbonate transport	-	-	-	Abnormalities of choroid plexus and ↓ in CSF volume and pressure in lateral ventricles. CSF abnormal ion chemistry. ↓ seizure threshold, abnormal retinal architecture & ERG [10]
SLC4A7 (SLC4A6, NBC3)	Many (brain low)	Regulates intracellular pH and may play a role in bicarbonate salvage in secretory epithelia	-	-	Autism? [11]	Mice lacking NBC3 developed blindness and auditory impairment because of degeneration of sensory receptors in the eye and inner ear as in Usher syndrome[12]
SLC4A8 (NDCBE KNBC3)	Brain Kidney	pH regulation in neurons	-	-	Autism? [11]	Reduced glutamate release in CA1 pyramidal layer + altered excitability[13] Effect on sodium reclamation in renal cortex collecting ducts[14]
SLC4A9 (AE4)	Kidney	anion exchanger of the kidney cortex	-	-	-	Affects transepithelial absorption of NaCl by renal intercalated cells[15]

Supplementary Table 2: *SLC4A10* variants identified in affected individuals in this study.

Variant	GRCh38 g.	GRCh37 g.	nucleotide change	NM_001178015 c.	Exon /27	SIFT (<0.05)	Polyphen (prob.)	REVEL	gnomAD v2.1.1	gnomAD v3.1.1
Predicted loss-of-function variants										
Trp140Argfs*39	2:161846109-161895992	2:162702619-162752502	del	417_1341del	5-11	NA	NA	NA	Absent	Absent
Arg757*	2:161949151	2:162805661	C>T	2269C>T	18	NA	NA	NA	Absent	Absent
Gln954_Phe955ins*13	2:161964133	2:162820643	A>C	2863-2A>C	Intron 21/26	NA	NA	NA	Absent	Absent
Trp873*	2:161957066	2:162813576	G>A	2619G>A	20	NA	NA	NA	Absent	Absent
Missense variants										
Lys577Met	2:161904888	2:162761398	A>T	1730A>T	14	damaging 0.048	probably damaging 0.985	0.873	Absent	Absent
Asn1103Ile	2:161976840	2:162833350	A>T	3308A>T	25	damaging 0.002	benign 0.197	0.239	Absent	Absent

Abbreviations: del, deletion; NA, not applicable; REVEL, rare exome variant ensemble learner; SIFT, sorting intolerant from tolerant

Supplementary Table 3: Variants identified by exome / genome sequencing.

Individual(s)	Variant (GRCh37)	Zygosity	Inh	Gene	Expression	OMIM phenotype	gnomAD v2.1.1 (AF)	REVEL	ClinVar	Interpretation
Family 1 III:1 and 2	Chr2(GRCh37):g.168105649G>A NM_152381.5:c.7747G>A; p.(Val2583Met)	hom	NK	*XIRP2*	Muscle; Low in brain	-	-	0.017	-	No disease association, low brain expression predicted benign
Family 1 III:1 and 2	Chr2(GRCh37):g.171256775_171256780del NM_138995.4:c.1869_1874del; p.(His624_Gln625del)	hom	NK	*MYO3B*	Low in brain	-	105 hets	-	-	No disease association, low brain expression
Family 1 III:1 and 2	Chr2(GRCh37):g.170010978A>G NM_004525.2:c.12287T>C; p.(Ile4096Thr)	hom	NK	*LRP2*	Kidney; Thyroid, Low in brain	Donnai-Barrow syndrome, 222448	109 hets	0.255	VUS	Published phenotype is absent, predicted benign
Family 1 III:1 and 2	Chr5(GRCh37):g.179160382C>G NM_014757.4:c.269C>G;p.(Pro90Arg)	hom	NK	*MAML1*	Widespread	-	-	0.066	-	No disease association, predicted benign
Family 1 III:1 and 2	Chr5(GRCh37):g.195286G>A NM_001080478.2:c.1363G>A; p.(Ala455Thr)	hom	NK	*LRRC14B*	Muscle; Low in brain	-	-	0.048	-	No disease association, low brain expression predicted benign
Family 1 III:1 and 2	Chr6(GRCh37):g.90333750C>T NM_014942.4:c.1192C>T; p.(Arg398Trp)	hom	NK	*ANKRD6*	Widespread	-	11 hets	0.397	-	No disease association
Family 1 III:1 and 2	Chr11(GRCh37):g.33566490A>C NM_012194.2:c.2060A>C; p.(Asn687Thr)	hom	NK	*KIAA1549L*	Brain	-	-	0.179	-	No disease association, predicted benign
Family 1 III:1 and 2	Chr11(GRCh37):g.118769236G>A NM_182557.2:c.4388C>T p.(Pro1463Leu)	hom	NK	*BCL9L*	Widespread	-	2 hets	0.272	-	No disease association
Family 1 III:1 and 2	Chr11(GRCh37):g.34144027A>G NM_024662.2:c.802A>G; p.(Ile268Val)	hom	NK	*NAT10*	Widespread	-	5 hets	0.204	-	No disease association, predicted benign
Family 1 III:1 and 2	Chr11(GRCh37):g.124056686C>G NM_001355213.1:c.710C>G; p.(Ala237Gly)	hom	NK	*OR10D3*	Testis; Low in brain	-	4 hets	0.235	-	No disease association, low brain expression
Family 1 III:1 and 2	Chr11(GRCh37):g.108385518C>G NM_015065.2:c.716G>C; p.(Arg239Thr)	hom	NK	*EXPH5*	Skin and cerebellum	Epidermolysis bullosa, nonspecific, autosomal recessive, 615028	137 hets	0.106	-	Published phenotype is absent
Family 1 III:1 and 2	Chr11(GRCh37):g.108409802A>T NM_015065.2:c.392T>A; p.(Phe131Tyr)	hom	NK				138 hets	0.125	-	Published phenotype is absent
Family 1 III:1 and 2	Chr12(GRCh37):g.55356369G>T NM_001098815.2:c.1313C>A; p.(Ala438Glu)	hom	NK	*TESPA1*	Brain	-	-	0.152	-	No disease association

Family 1 III:1 and 2	Chr12(GRCh37):g.49445208_49445234del NM_003482.3:c.2232_2258del; p.(Arg755_Pro763del)	hom	NK	*KMT2D*	Widespread	Kabuki syndrome 1, 147920	22 hets	-	VUS	inheritance is AD; parents are unaffected
Family 1 III:1 and 2	Chr22(GRCh37):g.32289717G>A NM_001136029.2:c.4156G>A; p.(Ala1386Thr)	hom	NK	*DEPDC5*	Widespread	Epilepsy, familial focal, with variable foci 1, 604364	18 hets	0.251	-	inheritance is AD; parents are unaffected
Family 1 III:1 and 2	ChrX(GRCh37):g.18283700C>G NM_006089.2:c.948+5G>C; p.?	hemi	NK	*SCML2*	Testis / Ovary, Low in brain	-	-	-	-	No disease association, low brain expression
Family 1 III:1 and 2	ChrX(GRCh37):g.47920225C>G NM_001037735.3:c.115G>C; p.(Glu39Gln)	hemi	NK	*ZNF630*	Widespread	-	-	0.205	-	No disease association
Family 1 III:1 and 2	ChrX(GRCh37):g.100401154T>C NM_006733.3:c.1714T>C; p.(Tyr572His)	hemi	NK	*CENPI*	Low in brain	-	-	0.076	-	No disease association, low brain expression, predicted benign
Family 1 III:1 and 2	Chr8(GRCh37):g.107749806G>A NM_001198532.1:c.2018G>A; p.(Arg673His)	het	NK	*OXR1*	Widespread	Cerebellar hypoplasia/atrophy, epilepsy, and global developmental delay, 213000	4 hets	0.398	-	All described cases have had biallelic loss-of-function variants
Family 1 III:1 and 2	Chr8(GRCh37):g.107763087C>G NM_001198532.1:c.2543C>G; p.(Ser848Cys)	het	NK				6 hets	0.298	-	
Family 1 III:1 and 2	Chr7(GRCh37):g.151845190G>A NM_170606.3:c.13822C>T; p.(Arg4608Cys)	het	NK	*KMT2C*	Widespread	Kleefstra syndrome 2, 617768	4 hets	0.217	-	Published phenotype is absent, one variant is predicted benign
Family 1 III:1 and 2	Chr7(GRCh37):g.151946979C>A NM_170606.3:c.1795G>T; p.(Asp599Tyr)	het	NK				39 hets	0.321	Not defined	
Family 1 III:1 and 2	Chr14(GRCh37):g.105609114G>A NM_145159.2:c.3521C>T; p.(Pro1174Leu)	het	NK	*JAG2*	Widespread	-	90 hets	0.169	-	No disease association, one variant predicted benign
Family 1 III:1 and 2	Chr14(GRCh37):g.105612780G>A NM_145159.2:c.2537C>T; p.(Ser846Phe)	het	NK			-	-	0.398	-	
Family 2 II:1	Chr3(GRCh37):g.148928067T>C NM_000096.4:c.494A>G; p.(Gln165Arg)	het	NK	*CP*	Liver	Hemosiderosis, systemic, due to aceruloplasminemia, 604290	-	0.423	-	Late onset disorder
Family 3 II:2 and 3	Chr2(GRCh37):g.182386959A>G NM_000885:c.1964A>G; p.(Lys655Arg)	hom	NK	*ITGA4*	Lymphocytes	-	-	0.208	-	Mouse KO exhibit embryonic lethality

Family 3 II:2 and 3	Chr2(GRCh37):g.225376319A>G NM_003590:c.655-20T>C	hom	NK	*CUL3*	Testis	Neurodevelopmental disorder with or without autism or seizures, 619239	4 hets	-	-	OMIM disorder is AD SpliceAI predicts no splicing change (0.01)
Family 3 II:2 and 3	Chr13(GRCh37):g.21099923G>T NM_015974:c.11C>A; p.(Ser4Tyr)	hom	NK	*CRYL1*	Liver, Kidney	-	11 hets	0.125	-	No disease association, predicted benign
Family 4 III:2 and III:3	Chr3(GRCh37):g.33661190C>T NM_001207044.1:c.523G>A; p.(Ala175Thr)	hom	NK	*CLASP2*	Widespread	-	2 hets	0.477	-	No disease association
Family 5 II:1 and 2	Chr1(GRCh37):g.19166140C>T NM_152232.2:c.2473G>A, p.(Ala825Thr)	hom	Bipar-ental	*TAS1R2*	Low, skin only	-	49 hets	0.242	-	Taste receptor No disease association

Abbreviations: -, absent; AD, autosomal dominant; hemi; hemizygous, het, heterozygous; hets, heterozygous individuals; hom, homozygous; OMIM, Online Mendelian Inheritance in Man; NK, not known; ProbD Probably damaging; PossD, possibly damaging; VUS, Variant of uncertain significance.

Supplementary Table 4: Summary of electrophysiological recording from acute brain slices of *Slc4a10* WT and knock-out (KO) mice.

	WT (n)	KO (n)	KO+TriMA (n)	t-test	one-way ANOVA with Newman-Keuls posthoc	KS-Test
capacitance (pF)	25.7±1.0 (22)	26.0±0.7 (31)		p=0.79		
input resistance (MΩ)	60.6±2.5 (22)	60.9±1.6 (31)		p=0.91		
mEPSCs						
amplitude (pA)	16.3±0.6 (10)	15.9±0.8 (12)		p=0.76		p>0.05
frequency (Hz)	1.2±0.3 (10)	0.9±0.1 (12)		p=0.40		p>0.05
T_{decay} (ms)	3.5±0.2 (10)	3.9±0.7 (12)		p=0.16		
charge transfer (pA*ms)	118.1±10.0 (10)	115.4±6.8 (12)		p=0.83		
mIPSCs						
amplitude (pA)	29.5±3.1 (12)	26.6±1.4 (19)	26.8±4.0 (11)		F=0.36, p=0.70; KO vs. WT p>0.05; WT vs. KO+TriMA: p>0.05	p>0.05
frequency (Hz	5.0±0.5 (12)	2.2±0.3 (19)	3.7±0.59 (11)		F=10.99, p=0.0002; KO vs. WT p<0.001; WT vs. KO+TriMA p>0.05	p<0.0001
T_{decay} (ms)	5.4±0.4 (12)	3.8±0.2 (19)	3.8±0.4 (11)		F=7.60, p=0.002; WT vs. KO p<0.001; KO vs. KO+TriMA p>0.05	
charge transfer (pA*ms)	199.2±20.1 (12)	143.3±9.8 (19)	145.8±20.9 (11)		F=4.58, p=0.016; KO vs. WT p<0.05; KO vs. KO+TriMA: p>0.05	
mIPSCs (HEPES)						
amplitude (pA)	27.0±2.1 (12)	27.3±2.4 (14)		p=0.93		
frequency (Hz	2.9±0.3 (12)	2.5±0.3 (14)		p=0.43		
T_{decay} (ms)	5.1±0.2 (12)	5.1±0.3 (14)		p=0.91		p>0.05
charge transfer (pA*ms)	206.4±21.5 (12)	210.2±22.0 (14)		p=0.90		p>0.05

Supplementary Table 5: SLC4A10 GWAS associations

A) associations with cognitive ability: MTAG: multi-trait analysis of genome-wide association studies

GRCh38 Chr:Pos	RsID	Risk allele	Site	P-Value	Effect si e ( )	Trait	Ref
2:161962111	rs4500960	T	Intronic	2×10^{-37}	0.021 unit	Highest math class taken (MTAG)	16
2:161962111	rs4500960	T	Intronic	3×10^{-30}	0.01 unit	Educational attainment (MTAG)	16
2:161962111	rs4500960	T	Intronic	7×10^{-26}	0.024 unit	Cognitive performance (MTAG)	16
2:161962111	rs4500960	T	Intronic	1×10^{-20}	0.013 unit	Educational attainment (years of education)	16
2:161962111	rs4500960	T	Intronic	3×10^{-11}	6.637 z-score	General cognitive ability	17
2:161962111	rs4500960	T	Intronic	3×10^{-10}	0.014 unit	Educational attainment (years of education)	18
2:161962111	rs4500960	C	Intronic	2×10^{-20}	0.021 unit	Highest math class taken	16
2:161971491	rs4664442	A	Intronic	5×10^{-17}	0.02 unit	Intelligence (MTAG)	19
2:161971491	rs4664442	?	Intronic	1×10^{-13}	0.01 unit	Cognitive ability, years of educational attainment or schizophrenia (pleiotropy)	20
2:161945674	rs11693702	A	Intronic	9×10^{-13}	0.021 unit	Cognitive performance	16
2:161957297	rs10221808	A	Intronic	3×10^{-10}	0.010 unit	Educational attainment (years of education)	16
2:161957297	rs10221808	?	Intronic	7×10^{-8}	-	Educational attainment (years of education)	21
2:161988766	rs2098526	A	Downstream	2×10^{-8}	0.0241 unit	Educational attainment (years of education)	16

B) associations with brain volume: DS: Downstream, TF site: Transcription factor site, CRE: cis-regulatory element

GRCh38 Chr:Pos	RsID	Risk allele	Site	P-Value	Effect si e ( )	Trait	Ref
2:161989055	rs1861979	T	TF site (DS)	9×10^{-22}	11.92 mm3	Hippocampal tail volume	22
2:161989055	rs1861979	T	TF site (DS)	5×10^{-13}	39. 4 mm3	Total hippocampal volume	22
2:161989055	rs1861979		TF site (DS)	2×10^{-10}	6.42 mm3	Dentate gyrus molecular layer volume	22
2:161989929	rs2909443	G	Downstream	3×10^{-13}	6.11 mm3	Hippocampal tail volume (corrected for total hippocampal volume)	22
2:161986568	rs2909455	T	CRE (DS)	6×10^{-11}	.4 mm3	Subiculum volume	22

C) associations with mental health outcomes: ADHD: attention deficit hyperactivity disorder, CBT: cognitive behavioral therapy

GRCh38 Chr:Pos	RsID	Risk allele	Site	P-Value	Effect size	Trait	Ref
2:161989345	rs2909457	G	Intronic	5×10^{-8}	OR 1.06	Schizophrenia	[23]
2:161989345	rs2909457	G	Intronic	6×10^{-8}	OR 1.06	Schizophrenia	[24]
2:161989345	rs2909457	?	Intronic	1×10^{-7}		Schizophrenia	[25]
2:161972220	rs34685708	?	Intronic	4×10^{-7}		Schizophrenia	[26]
2:161719475	rs56037433	?	Intronic	9×10^{-7}		Bipolar disorder or ADHD	[27]
2:161587424	rs79996792	A	Upstream	3×10^{-6}	0.019 unit	Neuroticism	[28]
2:161476919	rs12468729	G	Upstream	4×10^{-6}	OR 1.07	Bipolar disorder	[29]
2:161443775	rs13432654	?	Upstream	8×10^{-6}		Anxiety disorder, CBT	[30]

Supplementary References

1. Peters LL, Shivdasani RA, Liu SC*, et al*. Anion exchanger 1 (band 3) is required to prevent erythrocyte membrane surface loss but not to form the membrane skeleton. *Cell*. Sep 20 1996;86(6):917-27. doi:10.1016/s0092-8674(00)80167-1
2. Mumtaz R, Trepiccione F, Hennings JC*, et al*. Intercalated Cell Depletion and Vacuolar H(+)-ATPase Mistargeting in an Ae1 R607H Knockin Model. *Journal of the American Society of Nephrology : JASN*. May 2017;28(5):1507-1520. doi:10.1681/asn.2016020169
3. Huynh MT, Nguyen TT, Grison S, Lascols O, Fernandez E, Barbu V. Clinical characteristics and genetic profiles of young and adult patients with cholestatic liver disease. *Rev Esp Enferm Dig*. Oct 2019;111(10):775-788. doi:10.17235/reed.2019.6168/2019
4. Medina JF, Recalde S, Prieto J*, et al*. Anion exchanger 2 is essential for spermiogenesis in mice. *Proc Natl Acad Sci U S A*. Dec 23 2003;100(26):15847-52. doi:10.1073/pnas.2536127100
5. Thorsen K, Dam VS, Kjaer-Sorensen K*, et al*. Loss-of-activity-mutation in the cardiac chloride-bicarbonate exchanger AE3 causes short QT syndrome. *Nat Commun*. Nov 22 2017;8(1):1696. doi:10.1038/s41467-017-01630-0
6. Sander T, Toliat MR, Heils A*, et al*. Association of the 867Asp variant of the human anion exchanger 3 gene with common subtypes of idiopathic generalized epilepsy. *Epilepsy Res*. Oct 2002;51(3):249-55. doi:10.1016/s0920-1211(02)00152-3
7. Hentschke M, Wiemann M, Hentschke S*, et al*. Mice with a targeted disruption of the Cl-/HCO3- exchanger AE3 display a reduced seizure threshold. *Mol Cell Biol*. Jan 2006;26(1):182-91. doi:10.1128/mcb.26.1.182-191.2006
8. Prasad V, Bodi I, Meyer JW*, et al*. Impaired cardiac contractility in mice lacking both the AE3 Cl-/HCO3- exchanger and the NKCC1 Na+-K+-2Cl- cotransporter: effects on Ca2+ handling and protein phosphatases. *J Biol Chem*. Nov 14 2008;283(46):31303-14. doi:10.1074/jbc.M803706200
9. Igarashi T, Inatomi J, Sekine T*, et al*. Mutations in SLC4A4 cause permanent isolated proximal renal tubular acidosis with ocular abnormalities. *Nature genetics*. Nov 1999;23(3):264-6. doi:10.1038/15440
10. Kao L, Kurtz LM, Shao X*, et al*. Severe neurologic impairment in mice with targeted disruption of the electrogenic sodium bicarbonate cotransporter NBCe2 (Slc4a5 gene). *J Biol Chem*. Sep 16 2011;286(37):32563-74. doi:10.1074/jbc.M111.249961
11. Satterstrom FK, Kosmicki JA, Wang J*, et al*. Large-Scale Exome Sequencing Study Implicates Both Developmental and Functional Changes in the Neurobiology of Autism. *Cell*. Feb 6 2020;180(3):568-584.e23. doi:10.1016/j.cell.2019.12.036
12. Bok D, Galbraith G, Lopez I*, et al*. Blindness and auditory impairment caused by loss of the sodium bicarbonate cotransporter NBC3. *Nature genetics*. Jul 2003;34(3):313-9. doi:10.1038/ng1176
13. Sinning A, Liebmann L, Kougioumtzes A, Westermann M, Bruehl C, Hübner CA. Synaptic glutamate release is modulated by the Na+ -driven Cl- HC exchanger Slc4a8. *The Journal of neuroscience : the official journal of the Society for Neuroscience*. May 18 2011;31(20):7300-11. doi:10.1523/jneurosci.0269-11.2011
14. Leviel F, Hübner CA, Houillier P*, et al*. The Na+-dependent chloride-bicarbonate exchanger SLC4A8 mediates an electroneutral Na+ reabsorption process in the renal cortical collecting ducts of mice. *J Clin Invest*. May 2010;120(5):1627-35. doi:10.1172/jci40145
15. Chambrey R, Kurth I, Peti-Peterdi J*, et al*. Renal intercalated cells are rather energized by a proton than a sodium pump. *Proc Natl Acad Sci U S A*. May 7 2013;110(19):7928-33. doi:10.1073/pnas.1221496110
16. Lee JJ, Wedow R, Okbay A*, et al*. Gene discovery and polygenic prediction from a genome-wide association study of educational attainment in 1.1 million individuals. *Nature genetics*. Jul 23 2018;50(8):1112-1121. doi:10.1038/s41588-018-0147-3

17. Davies G, Lam M, Harris SE*, et al*. Study of 300,486 individuals identifies 148 independent genetic loci influencing general cognitive function. *Nat Commun*. May 29 2018;9(1):2098. doi:10.1038/s41467-018-04362-x
18. Okbay A, Beauchamp JP, Fontana MA*, et al*. Genome-wide association study identifies 74 loci associated with educational attainment. *Nature*. May 26 2016;533(7604):539-42. doi:10.1038/nature17671
19. Hill WD, Marioni RE, Maghzian O*, et al*. A combined analysis of genetically correlated traits identifies 187 loci and a role for neurogenesis and myelination in intelligence. *Molecular psychiatry*. 2019/02/01 2019;24(2):169-181. doi:10.1038/s41380-017-0001-5
20. Lam M, Hill WD, Trampush JW*, et al*. Pleiotropic Meta-Analysis of Cognition, Education, and Schizophrenia Differentiates Roles of Early Neurodevelopmental and Adult Synaptic Pathways. *Am J Hum Genet*. Aug 1 2019;105(2):334-350. doi:10.1016/j.ajhg.2019.06.012
21. Kichaev G, Bhatia G, Loh PR*, et al*. Leveraging Polygenic Functional Enrichment to Improve GWAS Power. *Am J Hum Genet*. Jan 3 2019;104(1):65-75. doi:10.1016/j.ajhg.2018.11.008
22. van der Meer D, Rokicki J, Kaufmann T*, et al*. Brain scans from 21,297 individuals reveal the genetic architecture of hippocampal subfield volumes. *Molecular psychiatry*. Nov 2020;25(11):3053-3065. doi:10.1038/s41380-018-0262-7
23. Ripke S, Neale BM, Corvin A*, et al*. Biological insights from 108 schizophrenia-associated genetic loci. *Nature*. 2014/07/01 2014;511(7510):421-427. doi:10.1038/nature13595
24. Goes FS, McGrath J, Avramopoulos D*, et al*. Genome-wide association study of schizophrenia in Ashkenazi Jews. *Am J Med Genet B Neuropsychiatr Genet*. Dec 2015;168(8):649-59. doi:10.1002/ajmg.b.32349
25. Periyasamy S, John S, Padmavati R*, et al*. Association of Schizophrenia Risk With Disordered Niacin Metabolism in an Indian Genome-wide Association Study. *JAMA Psychiatry*. Oct 1 2019;76(10):1026-1034. doi:10.1001/jamapsychiatry.2019.1335
26. Pardiñas AF, Holmans P, Pocklington AJ*, et al*. Common schizophrenia alleles are enriched in mutation-intolerant genes and in regions under strong background selection. *Nature genetics*. 2018/03/01 2018;50(3):381-389. doi:10.1038/s41588-018-0059-2
27. van Hulzen KJE, Scholz CJ, Franke B*, et al*. Genetic Overlap Between Attention-Deficit/Hyperactivity Disorder and Bipolar Disorder: Evidence From Genome-wide Association Study Meta-analysis. *Biol Psychiatry*. Nov 1 2017;82(9):634-641. doi:10.1016/j.biopsych.2016.08.040
28. Okbay A, Baselmans BM, De Neve JE*, et al*. Genetic variants associated with subjective well-being, depressive symptoms, and neuroticism identified through genome-wide analyses. *Nature genetics*. Jun 2016;48(6):624-33. doi:10.1038/ng.3552
29. Stahl EA, Breen G, Forstner AJ*, et al*. Genome-wide association study identifies 30 loci associated with bipolar disorder. *Nature genetics*. May 2019;51(5):793-803. doi:10.1038/s41588-019-0397-8
30. Coleman JR, Lester KJ, Keers R*, et al*. Genome-wide association study of response to cognitive-behavioural therapy in children with anxiety disorders. *Br J Psychiatry*. Sep 2016;209(3):236-43. doi:10.1192/bjp.bp.115.168229